SECURITY INFORMATION

CONFIDENTIAL

397

Copy
RM L52H13

NACA RM L52H13

NACA

RESEARCH MEMORANDUM

CONTROL HINGE-MOMENT AND EFFECTIVENESS CHARACTERISTICS OF A 60° HALF-DELTA TIP CONTROL ON A 60° DELTA WING AT MACH NUMBERS OF 1.41 AND 1.96

By Lawrence D. Guy

Langley Aeronautical Laboratory
Langley Field, Va.

CLASSIFICATION CHANGED TO UNCLASSIFIED
AUTHORITY: NACA RESEARCH ABSTRACT NO. 105
DATE: AUGUST 28, 1956
WHL

CLASSIFIED DOCUMENT

This material contains information affecting the National Defense of the United States within the meaning of the espionage laws, Title 18, U.S.C., Secs. 793 and 794, the transmission or revelation of which in any manner to unauthorized person is prohibited by law.

NATIONAL ADVISORY COMMITTEE
FOR AERONAUTICS

WASHINGTON

October 14, 1952

CONFIDENTIAL

NATIONAL ADVISORY COMMITTEE FOR AERONAUTICS

RESEARCH MEMORANDUM

CONTROL HINGE-MOMENT AND EFFECTIVENESS CHARACTERISTICS OF A 60° HALF-DELTA TIP CONTROL ON A 60° DELTA WING AT MACH NUMBERS OF 1.41 AND 1.96

By Lawrence D. Guy

SUMMARY

An investigation of a half-delta wing-tip control on a semispan 60° delta-wing—fuselage combination was conducted in the Langley 9- by 12-inch supersonic blowdown tunnel. The control spanned the outer one-third of the exposed wing semispan and had the hinge line located at the 45.5-percent station of the control mean aerodynamic chord. Control-surface hinge moments and bending moments, as well as the characteristics of the complete wing-fuselage combination, were obtained over a large range of control deflection and angle of attack at Mach numbers of 1.41 and 1.96 and Reynolds numbers of 2.4×10^6 and 2.0×10^6, respectively.

The control hinge moments were relatively small, for moderate angles of attack, over the entire control-deflection range of ±30°. At large angles of attack, however, large negative increases in hinge moment occurred with increasing absolute magnitude of the deflection. The values of the hinge-moment parameter, C_{h_δ}, at moderate angles of attack were considerably more positive at negative deflections than at positive deflections. This characteristic apparently was typical of control arrangements having tip-balance areas extending to the wing leading edge, as was shown to exist for three tip horn-balanced control configurations.

Because of the nonlinear nature of the hinge-moment curves, linear theory was of little value for predicting hinge moments except at small angles of attack and control deflection.

The control was effective throughout the range of the investigation which included angles of attack from 0° to 24° and angles of control deflection from -30° to 30° at a Mach number of 1.96.

The objectionable nonlinearities in the hinge-moment variations with both angle of attack and deflection at small angles were successfully eliminated by a fence located at the wing-control parting line. The fence increased the minimum drag of the wing but caused no drag increase at moderate and high lift coefficients at Mach numbers of 1.41 and 1.96.

INTRODUCTION

The half-delta wing-tip control has been shown to be an effective lateral-control device at transonic and supersonic speeds and, for the proper hinge-line location, to have relatively low hinge moments over a given Mach number range (refs. 1 to 4). Previous investigations were limited to low-angle conditions; it is therefore desirable to learn the behavior of this type of control at high angles of attack and control deflection, particularly since it is known that for delta wings the load distribution near the tip undergoes substantial changes as the angle of attack is increased from moderate to high values (ref. 5). In order to furnish such information, an investigation was conducted in the Langley 9- by 12-inch supersonic blowdown tunnel on a half-delta control located at the tip of a 60° delta wing, similar to those of references 2, 3, 4, and 6, at Mach numbers of 1.41 and 1.96 and Reynolds numbers of 2.4×10^6 and 2.0×10^6, respectively.

The aerodynamic characteristics of the complete model, as well as control hinge moments and bending moments, were obtained throughout a maximum control-deflection range of ±30° and at angles of attack as high as 24°. A fence, mounted at the wing-control parting line, was tested in an attempt to modify hinge-moment characteristics. Control moments and rolling effectiveness have been compared with calculated values. In order to give some indication of the effects of a fence on subsonic wing characteristics, lift, drag, and pitching-moment measurements obtained at a Mach number of 0.73 and a Reynolds number of 2.2×10^6 are also presented. A mathematical analysis of the optical system, used to measure control-surface hinge moments and bending moments, is included in the appendix.

SYMBOLS

C_L lift coefficient, $\frac{\text{Lift}}{qS}$

C_D drag coefficient, $\frac{\text{Drag}}{qS}$

C_m pitching-moment coefficient, $\frac{\text{Pitching moment}}{qS\bar{c}}$; pitching-moment reference axis located at $0.25\bar{c}$

$C_{l_{gross}}$ gross rolling-moment coefficient, $\frac{\text{Semispan wing rolling moment}}{2qSb}$; reference axis shown in figure 1

C_{BM_f} control bending-moment coefficient, $\frac{\text{Bending moment}}{qS_f b_f}$; reference axis is root chord of control surface

C_h control hinge-moment coefficient, $\frac{\text{Hinge moment}}{qS_f \bar{c}_f}$; reference axis is hinge line

$C_l, \Delta C_L, \Delta C_m$ increment in gross rolling-moment coefficient, lift coefficient, and pitching-moment coefficient due to deflection of the control surface

q free-stream dynamic pressure

S semispan wing area (including area blanketed by fuselage)

S_f control-surface area

c local wing chord

$\bar{c}$ mean aerodynamic chord of wing

$\bar{c}_f$ mean aerodynamic chord of control surface

b wing span (twice distance from rolling-moment reference axis to wing tip)

b_f control-surface span (distance from parting line to tip)

α angle of attack measured with respect to free stream

δ control-surface deflection measured with respect to wing-chord plane.

δ_{av} average control-surface deflection

R Reynolds number based on mean aerodynamic chord of wing

M Mach number

Subscripts:

α slope of curve of coefficient plotted against α;

$$\frac{dC_{BM_f}}{d\alpha}, \quad \frac{dC_h}{d\alpha}$$

δ slope of curve of coefficient plotted against δ;

$$\frac{dC_l}{d\delta}, \quad \frac{dC_h}{d\delta}, \quad \frac{dC_{BM_f}}{d\delta}$$

DESCRIPTION OF MODEL

The principal dimensions of the semispan-wing—fuselage combination are given in figure 1 and a photograph of the model is shown in figure 2. The wing was of delta plan form having 60° leading-edge sweepback and a corresponding aspect ratio of 2.3. An all-movable half-delta control surface was located at the wing tip.

The main wing panel, exclusive of the control surface, was of solid steel and had modified hexagonal airfoil sections of constant thickness. The thickness ratio varied from 2.4 percent at the model center line to 9.2 percent at the wing-control parting line. The leading edge was modified by a small nose radius. The leading-edge and trailing-edge wedge angles, measured parallel to the air stream, were 6.78° and 13.80°, respectively.

The half-delta control surface spanned the outer one-third of the exposed semispan and rotated about an axis in the wing-chord plane parallel to the pitch axis. The axis was located at the 45.5-percent station of the control-surface mean aerodynamic chord. The control surface had 3.0-percent-thick double-wedge airfoil sections in planes parallel to the free-stream direction with the leading edge modified by a small nose radius. Two controls of the same plan form and airfoil sections were used in the investigation, one made of beryllium copper and one of steel. A fence extending 21.8 percent of the local chord above and below the wing-chord plane near the leading edge and tapering to 12.8-percent chord at the trailing edge was mounted on the wing at the wing-control parting line for part of the investigation.

A fuselage consisting of a half body of revolution together with a 0.25-inch shim was integral with the main wing panel for all tests.

TUNNEL

The tests were conducted in the Langley 9- by 12-inch supersonic blowdown tunnel which uses the compressed air of the Langley 19-foot pressure tunnel. The absolute stagnation pressure of the air entering the test section ranges from 2 to $2\frac{1}{3}$ atmospheres. The compressed air is conditioned to insure condensation-free flow in the test section by being passed through a silica-gel drier and then through banks of finned electrical heaters. Criteria for condensation-free flow were obtained from reference 7. Turbulence damping screens were located in the settling chamber. Three test-section Mach numbers are provided by interchangeable nozzle blocks.

Deviations of flow conditions in the test section with tunnel clear, determined from extensive calibration tests and reported in reference 8, are presented in the following table along with properties of the conditioned air:

Variable	Nominal Mach number	
	1.41	1.96
Maximum deviation in Mach number	±0.02	±0.02
Maximum deviation in ratio of static to stagnation pressure, percent	±2.0	±2.2
Maximum deviation in ratio of dynamic to total pressure	±0.4	±0.3
Maximum deviation in stream angle, degrees	±.25	±.20
Maximum dewpoint temperature, °F	20	-20
Minimum stagnation temperature, °F	120	165

A few tests were made in an experimental nozzle operating at a subsonic Mach number of 0.73. Details of the flow characteristics of this nozzle were unknown, but wall pressure measurements indicated the tunnel-clear test-section Mach number variation was about ±0.01. The average subsonic test-section Mach number decreased about 0.02 as the angle of attack increased from 0° to 25°. The flow conditions were

believed to be sufficiently uniform to permit evaluation of changes in wing characteristics caused by addition of a fence to the wing.

TEST TECHNIQUE

The model was cantilevered from a five-component strain-gage balance set flush with the tunnel floor. The model and the balance rotated together as the angle of attack was changed. The aerodynamic forces and moments on the semispan-wing—fuselage combination were measured with respect to the body axes and then rotated to the wind axes. The fuselage consisted of a half body of revolution mounted on a 0.25-inch shim; the shim was used to minimize the tunnel boundary-layer effects on the flow over the circular portion of the fuselage (ref. 9). A clearance gap of 0.010 to 0.020 inch was maintained between the fuselage shim and the tunnel floor.

The hinge moments and bending moments on the tip control surface were measured by means of an optical system which was developed for use with wings too thin to permit conventional strain-gage installation. Light from high-intensity sources was reflected by mirrors imbedded flush with the model surfaces onto a circular-arc screen of 80-inch radius, 130-inch length, and 19-inch width. Clear plastic windows permitted passage of the light through the nozzle walls over a limited angle-of-attack range for a given light-source and mirror arrangement. The two mirrors required were adjacent to each other, one in the inner wing panel and one in the tip control, as shown in figure 1. Deflection of the control relative to the wing could then be measured by the relative positions on the screen of the light images reflected by the two mirrors. At several angles of attack for each control deflection with the model in place, static calibrations were made of the displacement of the light-image positions on the screen as functions of known values of hinge moments and bending moments applied to the control surface. By use of these calibrations the control hinge moments and bending moments were determined from light-image positions recorded during wind-on tests.

Duplicate control surfaces were used in the investigation. All the control-surface hinge-moment and bending-moment data and part of the five-component wing data were obtained with a control made of beryllium copper; the rest of the five-component wing data were obtained with a control made of steel. No appreciable differences were found to exist between data obtained for the two controls. In no instance did the control loads cause stresses in the controls approaching the yield point.

ACCURACY OF DATA

An estimate of the probable errors introduced in the present data by instrument-reading errors, measuring-equipment errors, and calibration errors are presented in the following table:

Variable	Moderate load conditions	Maximum load conditions
α	$\pm 0.02^{\circ}$	$\pm 0.05^{\circ}$
δ	$\pm .2^{\circ}$	$\pm .2^{\circ}$
C_l	$\pm .0005$	$\pm .0015$
C_L	$\pm .005$	$\pm .010$
C_D	$\pm .001$	$\pm .003$
C_m	$\pm .001$	$\pm .003$
C_h	$\pm .008$	$\pm .010$
C_{BM_f}	$\pm .015$	$\pm .020$

The inaccuracies in the measurement of control hinge moment and bending moment are attributed to: erratic effects of friction between the bearing in the wing panel and the shaft of the control; errors in the calibrations wherein loads were applied by means of a hand-held stylus; the fact that the distortion of the control under an aerodynamic load is not the same as the distortion under a calibration load; and errors arising from certain relations in the optics of the measuring system. This last source of error is discussed in greater detail subsequently.

At the time the present investigation was begun, interest lay primarily in control hinge moments. A preliminary analysis of the optical system showed that the hinge moments could be obtained by direct use of a static calibration when certain conditions were imposed on the light-source and mirror arrangement. These conditions required the light-source—mirror system (the striking ray, the reflected ray, and the line normal to the mirror surface) for both wing and control mirrors to be coplanar and perpendicular to the hinge line for all angles of attack and deflection. Although these conditions were not exactly met, calculations based on the detailed analysis of the appendix have shown that resulting errors were negligible.

In addition to hinge moments, bending moments also were obtained because their measurement involved little extra labor. Calculations have shown that the errors in bending moment resulting when the light-mirror systems were not being exactly coplanar and perpendicular to the

hinge line were negligible; however, the analysis in the appendix shows that, when the angles between the striking ray and normal for the wing and control were not equal and when the normals were not coincident, bending moments could not be obtained by direct use of the static calibrations. The required corrections were measurable but could not be applied to the present data because the necessary measurements of the numerous light-source positions were not made at the time of the tests. Thus, the error in bending moment is somewhat larger than that which would exist with the optical system if the corrections were taken into account.

A check on the over-all accuracy of the hinge-moment and bending-moment measurements was given by data obtained in overlapping regions where moments were obtained for the same model conditions but different light-source arrangements. On the basis of the repeated data, it appears that the estimates of probable errors in C_{BM_f} and C_h given by the preceding tables are reasonable.

It is evident that the accuracy of the present hinge-moment and bending-moment data does not warrant exact quantitative evaluation of the results, particularly when the control loadings are small. In order to provide an indication of the reliability of the data at small angles of attack and control deflection the control hinge moments and bending moments obtained by this system are compared in figure 3 with those obtained over a limited angle range in the investigation of reference 4. In the investigation of reference 4, control-surface loads of a wing-control arrangement which is the same as that of the subject report except for differences in size were transmitted by an internal staff which extended through a spanwise slot in the main wing panel to an electrical strain-gage balance. As considerable scatter existed in the data of reference 4, only the faired curves have been reproduced in figure 3. Although the accuracy of the measurements for both sets of data was of the same order, it should be pointed out that the sources of error in the two different systems are of a completely different nature. The data of figure 3 show that the hinge moments measured by the optical system and by the strain-gage balance were in excellent agreement except at zero deflection where a change in hinge-moment sign occurred at an angle of attack 3° higher for the optical system. The agreement between bending-moment measurements by the two systems, while not so good, was still reasonable.

RESULTS AND DISCUSSION

Figure 4 presents the basic aerodynamic coefficients of the wing-fuselage combination and of the half-delta tip control at a Mach number of 1.96 plotted against angle of attack for various control deflection angles. The deflection angles given in figures 4(a) to 4(d) for the

complete wing data are essentially constant throughout the angle-of-attack range. For the control-moment data of figures 4(e) and 4(f) average values of control deflection are shown and exact values are given in table I. These data at $M = 1.96$ are representative of those obtained at $M = 1.41$; therefore, the data at the lower Mach number have been presented only in the form of cross plots, along with the $M = 1.96$ data in subsequent figures, and a limited amount of data is presented for $M = 1.62$.

Control Bending-Moment and Hinge-Moment Characteristics

Figure 5 presents control hinge-moment and bending-moment coefficients cross-plotted against control deflection and hinge-moment coefficients plotted against angle of attack at Mach numbers of 1.41 and 1.96. Some of the data of figure 5 were obtained by reversing signs of test values of α, δ, C_h, and C_{BM}. This was desirable because the range of values of α and δ covered in the tests was limited by the movement of the light images of the optical system. The data thus obtained are applicable because the model is symmetrical.

Control bending moment.- With the fence off, the variation of bending moment with control deflection (fig. 5) was nearly linear for all angles of attack shown. For a given value of control deflection, however, the increase in bending moment per unit angle of attack progressively decreases as the angle of attack is increased to about 12° and then remains essentially constant with further increases in angle of attack (also see fig. 4(e)).

Control hinge moment, fence off.- For angles of attack less than 12°, the magnitudes of the hinge moments were small (fig. 5) which indicated that the tip control was reasonably well-balanced even at the largest control deflections tested ($\pm 30°$). For angles of attack greater than 12° (available only at $M = 1.96$), however, beginning at positive control deflections large negative increases in hinge moment with increasing deflection occurred. The hinge-moment coefficients were generally negative for positive values of α and δ indicating that the control was somewhat underbalanced (the center of pressure was behind the hinge line); for some small positive angle conditions, however, positive values of hinge moment indicated that the center of pressure was located ahead of the hinge line. The hinge-moment parameters C_{h_α} and C_{h_δ} were generally negative for positive values of α and δ.

For negative control deflections and all positive angles of attack except those near zero, the hinge moments with the fence off were negative and the values of C_{h_δ} were positive. Data to substantiate these results are not available for other tip controls of this type at sizeable angles of attack and deflection. Trailing-edge controls, having

tip horn-balance areas extending from the hinge line to the wing leading edge or beyond, however, might be expected to have similar characteristics. Hinge-moment data for such horn-balanced controls for moderate to high-angle conditions were obtained in the investigation of reference 10 and in another investigation (as yet unpublished) in this facility. In both investigations hinge moments were measured by means of electrical strain gages. For direct comparison, data for all controls, including the half-delta tip control, were reduced to coefficient form by using the control area and control mean aerodynamic chord behind the hinge line. These data presented in figure 6 substantiate the trends of the hinge-moment variation with deflection observed with the all-movable tip control. The positive shift of C_{h_δ} which occurs at moderate angles of attack as control deflection changes in a negative direction appears to be typical of control arrangements having tip-balance areas extending to the wing leading edge.

Some form of couple was acting on the control in some cases since substantial negative hinge moments were evident when bending moments were zero (fig. 5). The existence of such a couple can be illustrated by considering the variation of bending moment with angle of attack when the control is required to remain parallel with the free air stream (that is, control deflection and angle of attack are equal but of opposite sign). For this condition, bending moment increased (although at a decreasing rate) as angle of attack increased from 0° ($\delta = 0^\circ$) to 12° ($\delta = -12^\circ$), probably because of upwash from the inner wing panel. With further increase in angle of attack (available only at $M = 1.96$), the bending moment decreased until it became zero at 24° angle of attack and, at this angle, the hinge moment was large and negative. The control forces in this case were possibly affected by the air flow through the parting line ahead of the hinge line or it may have been that the influence of the shock field from the wing leading edge acted in opposition to the upwash effects of the inner wing panel. Detailed pressure distribution tests and flow studies would be required, however, to determine the exact cause of these unusual control-surface characteristics.

Control hinge moment, fence on.- At small angles of attack and deflection the nonlinear variations of hinge moment with deflection (fig. 5), which occurred for the basic configuration, were believed to be associated with flow through the opening resulting from the deflection of the control relative to the wing. The fence, which was installed at the parting line, successfully eliminated not only most of the nonlinear variations with deflection but also the nonlinear variations of hinge moment with angle of attack even with the control undeflected. As a result, C_{h_α} at zero angle of attack and deflection was reduced to a value more negative than that of C_{h_δ}. This change in C_{h_α} was in the direction which would be predicted by theory if the fence were of sufficient size to cause the control loading to behave in the same manner as that of an isolated wing. The hinge-moment parameter C_{h_δ} was essentially unchanged at zero angle of attack and deflection by

addition of the fence. Contrary to fence-off data, however, C_{h_δ} with fence on was generally negative at all angles of attack throughout the deflection range for which data were available. The positive shift in C_{h_δ} noted for the fence-off condition at negative deflections was apparently delayed to higher angles of attack and more negative deflections although, unfortunately, data for the negative deflection range were incomplete.

Comparison with linear theory.- The variation of the hinge-moment and bending-moment parameters C_{h_α}, C_{h_δ}, $C_{BM_{f_\alpha}}$, and $C_{BM_{f_\delta}}$ with Mach number at zero angle of attack and deflection is summarized in figure 7. Calculated values of these parameters, as obtained from linear theory (refs. 11 and 12) for the basic configuration are also presented in figure 7.

The calculated values of the bending-moment parameters $C_{BM_{f_\alpha}}$ and $C_{BM_{f_\delta}}$ were in reasonably good agreement with measured values. The measured values of these parameters decreased with increasing Mach number at a slightly more rapid rate than theory indicated.

Linear theory is of little value in predicting hinge moments for this type of balanced, all-movable tip control because of the nonlinear variation of hinge moment with both angle of attack and control deflection which occur at small values of α and δ. This variation is clearly illustrated by figures 5 and 7. Figure 7 shows that values of C_{h_α} for zero angle of attack and zero deflection were in good agreement with theory from Mach numbers 1.41 to 1.96. Figure 5, however, shows that C_{h_α} changed sign at a small angle of attack and generally had negative values up to the highest angles of attack tested.

Control Effectiveness Characteristics

Figure 8 presents the variation with control deflection of wing rolling moment, lift, and pitching-moment characteristics for Mach numbers of 1.41 and 1.96, with and without fence. Data were obtained at $M = 1.62$ but are not presented because linear interpolation between the data at $M = 1.41$ and $M = 1.96$ were within the experimental accuracy of the data at $M = 1.62$. Calculated rolling-moment effectiveness C_{l_δ} obtained from linear theory is also given for the fence-off condition. With fence off at zero angle of attack the variations of rolling moment, lift, and pitching moment with deflection were linear for small deflections and the change of rolling moment with deflection was in reasonably good agreement with theory. Increasing the magnitude of the angle of attack or deflection

from the low-angle range tended to decrease the parameters C_{l_δ}, ΔC_L, and ΔC_m. The decrease was not too pronounced for negative deflections even at the largest angles of attack or for positive deflections at zero angle of attack. In the positive deflection range as angle of attack was increased, however, the decrease became progressively more pronounced until a point was reached where further increases in deflection caused no further increases in rolling moment, lift, or pitching moment. The effect on these control parameters of adding the fence appeared to be somewhat erratic.

Effect of Fence on Wing Characteristics

The effects of a fence on the lift, drag, and pitching moment of the wing-fuselage combination with control undeflected are illustrated in figure 9 for Mach numbers of 0.73, 1.41, and 1.96.

The fence caused an increase in the values of minimum drag coefficient of about 0.003 at all Mach numbers. Repeat tests made at a later date to check the drag data were in agreement with the data shown. The increment in drag attributed to the fence at a Mach number of 0.73 was essentially constant up to values of lift coefficient of 0.35 at which point the presence of the fence caused an abrupt decrease in lift-curve slope which resulted in a corresponding increase in fence drag with further increases in lift coefficient. It is interesting to note that at supersonic Mach numbers, however, above a particular value of lift coefficient, the fence caused an increase in lift-curve slope. This increase in turn caused the fence drag penalty to vanish at values of lift coefficient of 0.50 and 0.35 at $M = 1.41$ and $M = 1.96$, respectively. Above a lift-coefficient value of 0.35 at $M = 1.96$ the drag of the model was actually less with the fence on than with the fence off.

CONCLUDING REMARKS

An investigation of a half-delta tip control on a 60° delta wing in the Langley 9- by 12-inch supersonic blowdown tunnel at Mach numbers of 1.41 and 1.96 indicated the following results:

The control, with a hinge line located at the 45.5-percent station of the control mean aerodynamic chord, exhibited relatively small hinge moments over the entire control-deflection range of ±30° for angles of attack less than 12°. At larger angles of attack (available only at a Mach number of 1.96) sizeable negative increases in hinge moment with increasing deflection occurred.

The values of the hinge-moment parameter C_{h_δ} at moderate angles of attack were considerably more positive at negative deflections than at positive deflections. This characteristic apparently was typical of control arrangements having tip-balance areas extending to the wing leading edge as was shown to exist for three tip horn-balanced control configurations.

Because of the nonlinear nature of the hinge-moment curves, the theory was of little value for predicting hinge moments except at very small angles of attack and deflection.

The control was effective throughout the range of the investigation which included angles of attack from 0° to 24° and angles of control deflection from -30° to 30° at a Mach number of 1.96.

An outboard fence successfully eliminated, at small angles, the objectionable nonlinear variations of hinge moment with both control deflection and angles of attack. The fence increased the value of the wing minimum drag coefficient by about 0.003 but also increased the wing lift-curve slope at moderate angles of attack at Mach numbers of 1.41 and 1.96, thereby causing the drag penalty to vanish.

Langley Aeronautical Laboratory,
National Advisory Committee for Aeronautics,
Langley Field, Va.

APPENDIX

ANALYSIS OF AN OPTICAL SYSTEM DEVELOPED TO MEASURE HINGE MOMENTS AND BENDING MOMENT OF CONTROLS ON THIN WINGS

By Kennith L. Goin

Hinge moments and bending moments of a control surface may be expressed in terms of deflection of the control with respect to the wing when the control is flexibly supported in position. The control deflection may in turn be determined from the movement on a screen of a light image reflected by a mirror in the control surface relative to the movement of a light image reflected from a second mirror in the wing. It is first necessary, however, to determine what part of the control-image movement is due to deflection of the wing under load since a one-to-one ratio would not necessarily exist between the wing-image movement and the movement of the control image due to wing deflection. Also, the correspondence of the light-image movement to the movement of the mirror must be established. The following detailed analysis determines these relations for the optical system developed for use in the Langley 9- by 12-inch supersonic blowdown tunnel: The analysis initially deals with an optical system in which the locations of the light sources and the attitudes of the mirrors are arbitrary.

The general arrangement of the optical system is shown in figure 10. The wing-control model was mounted vertically in the tunnel (shown with nozzle blocks removed) and the surface of the large circular image screen was parallel to the model pitch axis. For convenience of notation, an orthogonal coordinate system has been chosen such that the origin is at the mirror, the y-axis is parallel to the pitch axis of the model, and the yz-plane contains the light source. The intersection of the xz-plane with the image screen is the circular arc abc. The angles θ_i and θ_n are measured in the xz-plane and the angles γ_s, γ_n, and γ_i are measured from the y-axis in vertical planes containing the y-axis. From the fundamental properties of mirrors (the striking ray, the reflected ray, and line normal to mirror surface lie in a plane and the angle of incidence of the striking ray equals the angle of reflection) the following relations were obtained:

$$\theta_i = \tan^{-1} \frac{2m \sin \theta_n}{2m \cos \theta_n - p} \qquad (A1)$$

$$\gamma_i = \operatorname{ctn}^{-1} \frac{2m \operatorname{ctn} \gamma_n - p \operatorname{ctn} \gamma_s}{\sqrt{4m^2 - 4mp \cos \theta_n + p^2}} \tag{A2}$$

where

$$m = \cos \theta_n + \operatorname{ctn} \gamma_s \operatorname{ctn} \gamma_n$$

$$p = 1 + \operatorname{ctn}^2 \gamma_n$$

Any movement of the mirror is completely described by rotating about the y-axis (wing or control twist) and tilting with respect to the y-axis (wing or control bending). These movements can be defined by changes in the angles θ and γ of the mirror normal. The partial derivatives of equations (A1) and (A2) describe the angular change of the reflected ray due to deflection of the mirror normal and are as follows:

$$\frac{\partial \theta_i}{\partial \theta_n} = 2\left(\frac{2m^2 - mp \cos \theta_n + p \sin^2 \theta_n}{4m^2 - 4mp \cos \theta_n + p^2}\right) \tag{A3}$$

$$\frac{\partial \theta_i}{\partial \gamma_n} = \frac{-2p \sin \theta_n (2m \operatorname{ctn} \gamma_n - p \operatorname{ctn} \gamma_s)}{4m^2 - 4mp \cos \theta_n + p^2} \tag{A4}$$

$$\frac{\partial \gamma_i}{\partial \theta_n} = \frac{2 \operatorname{ctn} \gamma_n \sin \theta_n}{\sqrt{4m^2 - 4mp \cos \theta_n + p^2}} \tag{A5}$$

$$\frac{\partial \gamma_i}{\partial \gamma_n} = \frac{4m - 2p \cos \theta_n}{\sqrt{4m^2 - 4mp \cos \theta_n + p^2}} \tag{A6}$$

The preceding equations also may be used to describe the distance the light image travels on the screen. For small deflections of the mirror, such as those resulting from deflection under load, it is reasonable to assume that the screen is a plane normal to the reflected ray since γ_i is close to 90° and the screen radius is large (80 in.).

The angles of the light-image path on the screen, due to deflection of the mirror normal, with respect to the intersection of the xz-plane and the screen are then

$$\psi_{i\theta} = \tan^{-1} \frac{\partial\gamma_i/\partial\theta_n}{\partial\theta_i/\partial\theta_n} \tag{A7}$$

$$\psi_{i\gamma} = \tan^{-1} \frac{\partial\gamma_i/\partial\gamma_n}{\partial\theta_i/\partial\gamma_n} \tag{A8}$$

where the second subscript denotes the direction of movement of the mirror normal to which the angle ψ is due.

The previous discussion has been limited to development of the mechanics of a system of one light, mirror, and image. In the present tests there are two such systems, one for the control and one for the wing. The deflection of the control with respect to the wing is desired since this relative deflection is an indication of the control-surface loads. In order to determine the control deflection with respect to the wing, it is necessary to determine what part of the control deflection is due to wing deflection.

When the mirror in the wing rotates about the y-axis, the mirror in the control rotates about the y-axis an equal amount; that is, the change in θ_n of the tip control is equal to the change in θ_n of the wing. Thus,

$$\left(\Delta\theta_n\right)_t = \left(\Delta\theta_n\right)_w \tag{A9}$$

and

$$\frac{\left(\partial\gamma_n\right)_t}{\left(\partial\theta_n\right)_w} = 0 \tag{A10}$$

where subscripts t and w refer, respectively, to the control and wing.

When the wing mirror normal and the control mirror normal do not lie in the same vertical plane, a change in γ_n (bending) of the wing

does not cause an equal change in γ_n of the tip control. For example, in the extreme case, where the horizontal angle between wing and control mirror normals is 90° and γ_n of wing and control mirror normals are equal, a change in γ_n of the wing mirror causes simply a rotation of the control mirror about its own normal. The relations between the movements of the wing and tip normals are

$$\frac{\left(\partial\gamma_n\right)_t}{\left(\partial\gamma_n\right)_w} = \cos\rho \tag{A11}$$

and

$$\frac{\left(\partial\theta_n\right)_t}{\left(\partial\gamma_n\right)_w} = \sin\rho\left(\operatorname{ctn}\gamma_n\right)_t \tag{A12}$$

where ρ is the horizontal angle between the mirror normals $\left(\theta_{n_w} - \theta_{n_t}\right)$ if the wing and control light sources are in the same vertical plane. Summarizing equations (9) to (12) graphically yields

Wing normal movement:

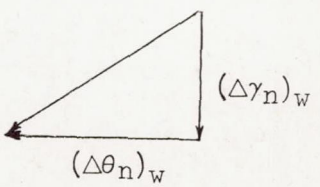

Corresponding tip normal movement:

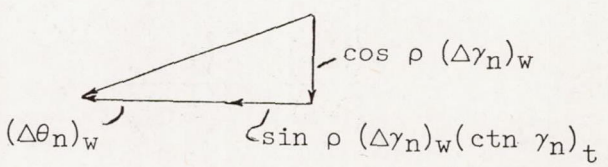

Normally the location of the light source and the reflected image will be known for both wing and control systems. Equations (A1) and (A2) allow solution for the location of the mirror normals. From the movement of the wing image due to model loads the deflection of the wing mirror normal may be obtained by use of equations (A3) to (A8).

From equations (A9) to (A12) the deflection of the control mirror normal corresponding to the wing deflection may be found. Again, using equations (A3) to (A8), the movement of the control image corresponding to wing deflection may be determined. The remaining movement of the control image is due only to the control-surface loads.

It is immediately evident that, in the general case just described, the calculations for each data point would involve a great deal of labor. For this reason such arrangements are not considered practical.

The preceding equations may be greatly simplified for wing-control arrangements in which the two light-mirror systems are coplanar and perpendicular to the hinge line for all angles of attack and control deflection. That is,

$$\gamma_{i_w} = \gamma_{n_w} = \gamma_{s_w} = \gamma_{i_t} = \gamma_{n_t} = \gamma_{s_t} = 90^\circ \tag{A13}$$

Therefore, the movement of the image from the control mirror due to deflection of the wing in bending becomes

$$\left(d\gamma_n\right)_w \frac{\left(\partial\theta_i\right)_t}{\left(\partial\gamma_n\right)_w} = 0 \tag{A14}$$

$$\left(d\gamma_n\right)_w \frac{\left(\partial\gamma_i\right)_t}{\left(\partial\gamma_n\right)_w} = \frac{\cos(\theta_n)_t}{\cos(\theta_n)_w} \cos\, \rho(\Delta\gamma_i)_w \tag{A15}$$

and the movements of the control and wing images due to wing twist are equal,

$$\frac{\left(\partial\theta_i\right)_t}{\left(\partial\theta_n\right)_w} = \frac{\left(\partial\theta_i\right)_w}{\left(\partial\theta_n\right)_w} \tag{A16}$$

From these relations the movement of the control image due only to control-surface loads can be found very simply. It should be noted that the wing-control arrangement of the present investigation approximates the conditions of equation (A13). An illustration of the breakdown into components of the wing- and control-image movements for this case are presented in figure 11.

The light-mirror relations may be further simplified if the wing- and control-mirror normals can be considered coincident and a single light source is used in that a one-to-one ratio then exists between the movement of the wing mirror image and the movement of the control mirror image due to wing movement. This simplification has the disadvantages that, in practice, the control mirror must be reset each time the control deflection is changed and the model surfaces will not be smooth when the control is deflected.

REFERENCES

1. Stone, David G.: Comparisons of the Effectiveness and Hinge Moments of All-Movable Delta and Flap-Type Controls on Various Wings. NACA RM L51C22, 1951.

2. Sandahl, Carl A., and Strass, H. Kurt: Comparative Tests of the Rolling Effectiveness of Constant-Chord, Full-Delta, and Half-Delta Ailerons on Delta Wings at Transonic and Supersonic Speeds. NACA RM L9J26, 1949.

3. Martz, C. William, Church, James D., and Goslee, John W.: Free-Flight Investigation To Determine Force and Hinge-Moment Characteristics at Zero Angle of Attack of a 60° Sweptback Half-Delta Tip Control on a 60° Sweptback Delta Wing at Mach Numbers Between 0.68 and 1.44. NACA RM L51I14, 1951.

4. Conner, D. William, and May, Ellery B., Jr.: Control Effectiveness Load and Hinge-Moment Characteristics of a Tip Control Surface on a Delta Wing at a Mach Number of 1.9. NACA RM L9H05, 1949.

5. Boyd, John W., and Phelps, E. Ray: A Comparison of the Experimental and Theoretical Loading Over Triangular Wings at Supersonic Speeds. NACA RM A50J17, 1951.

6. Martz, C. William, and Church, James D.: Flight Investigation at Subsonic, Transonic, and Supersonic Velocities of the Hinge-Moment Characteristics, Lateral-Control Effectiveness, and Wing Damping in Roll of a 60° Sweptback Delta Wing With Half-Delta Tip Ailerons. NACA RM L51G18, 1951.

7. Burgess, Warren C., Jr., and Seashore, Ferris L.: Criterions for Condensation-Free Flow in Supersonic Tunnels. NACA TN 2518, 1951.

8. May, Ellery B., Jr.: Investigation of the Effects of Leading-Edge Chord-Extensions on the Aerodynamic and Control Characteristics of Two Sweptback Wings at Mach Numbers of 1.41, 1.62, and 1.96. NACA RM L50L06a, 1951.

9. Conner, D. William: Aerodynamic Characteristics of Two All-Movable Wings Tested in the Presence of a Fuselage at a Mach Number of 1.9. NACA RM L8H04, 1948.

10. Mason, Maxwell, and Miller, Robert C.: Wind-Tunnel Test of 11 Per Cent Scale Semispan Models of the Douglas Nike 484 Missile. Rep. No. SWT 12-8, Jet Propulsion Lab., C.I.T., 1950.

11. Lagerstrom, P. A., and Graham, Martha E.: Linearized Theory Supersonic Control Surfaces. Jour. Aero. Sci., vol. 16, no. 1, Jan. 1949, pp. 31-34.

12. Malvestuto, Frank S., Jr., Margolis, Kenneth, and Ribner, Herbert S.: Theoretical Lift and Damping in Roll at Supersonic Speeds of Thin Sweptback Tapered Wings With Streamwise Tips, Subsonic Leading Edges, and Supersonic Trailing Edges. NACA Rep. 970, 1950. (Supersedes NACA TN 1860.)

TABLE I

VALUES OF ANGLE OF ATTACK AND CONTROL DEFLECTION FOR

DATA PRESENTED IN FIGURES 4(e) AND 4(f) M = 1.96

α, deg	Average δ, deg							
	-30.0	-20.3	-11.0	0	5.4	10.4	15.5	29.9
-10.11	-----	-----	-----	---	---	----	15.8	30.2
-8.05	-----	-----	-----	---	5.6	10.6	15.8	30.2
-6.02	-----	-----	-----	0.0	5.4	10.5	15.7	30.1
-4.00	-----	-----	-----	.0	5.4	10.4	15.6	30.1
-2.00	-----	-----	-----	.0	5.4	10.4	15.6	30.0
0.00	-----	-----	-----	.0	5.4	10.4	15.6	30.0
2.00	-----	-----	-----	.1	5.4	10.4	15.5	30.0
4.00	-----	-----	-10.8	.0	5.4	10.4	15.5	30.0
6.00	-----	-----	-10.9	.0	5.3	10.4	15.5	30.0
7.98	-----	-----	-10.9	.0	5.3	10.4	15.5	30.0
9.96	-----	-----	-11.0	-.1	5.3	10.3	15.5	29.9
11.94	-----	-20.2	-11.0	-.1	5.3	10.3	15.5	29.8
13.94	-----	-20.2	-11.0	---	---	10.3	15.5	29.7
15.94	-----	-20.3	-11.0	-.1	---	10.3	15.5	29.6
17.96	-----	-20.3	-11.0	-.2	---	10.2	15.4	29.5
19.99	-30.0	-20.3	-11.0	-.2	---	10.2	15.4	29.4
22.04	-30.0	-20.3	-11.0	-.2	---	10.2	15.4	29.4
24.12	-30.0	-20.3	-11.1	-.2	---	10.2	15.3	----
26.24	-30.0	-20.3	-11.1	-.2	---	----	15.2	----
28.43	-30.0	-20.3	-----	-.3	---	----	15.1	----
30.73	-30.0	-20.4	-----	-.4	---	----	15.0	----

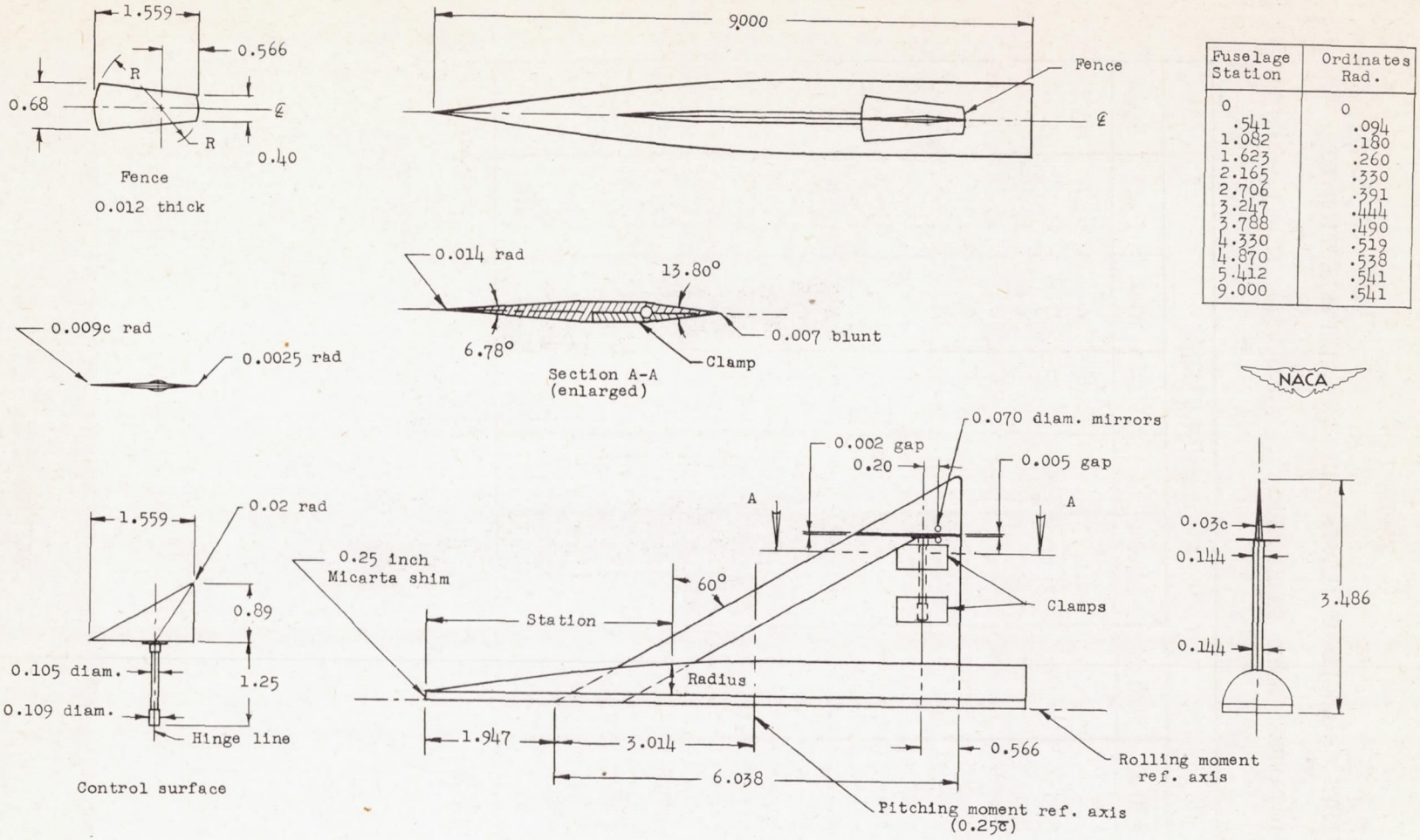

Fuselage Station	Ordinates Rad.
0	0
.541	.094
1.082	.180
1.623	.260
2.165	.330
2.706	.391
3.247	.444
3.788	.490
4.330	.519
4.870	.538
5.412	.541
9.000	.541

Figure 1.- Details of semispan-wing—fuselage combination. Aspect ratio, 2.3; mean aerodynamic chord, 4.025 in.; semispan, 3.486 in.; half-wing area, 10.524 sq in.

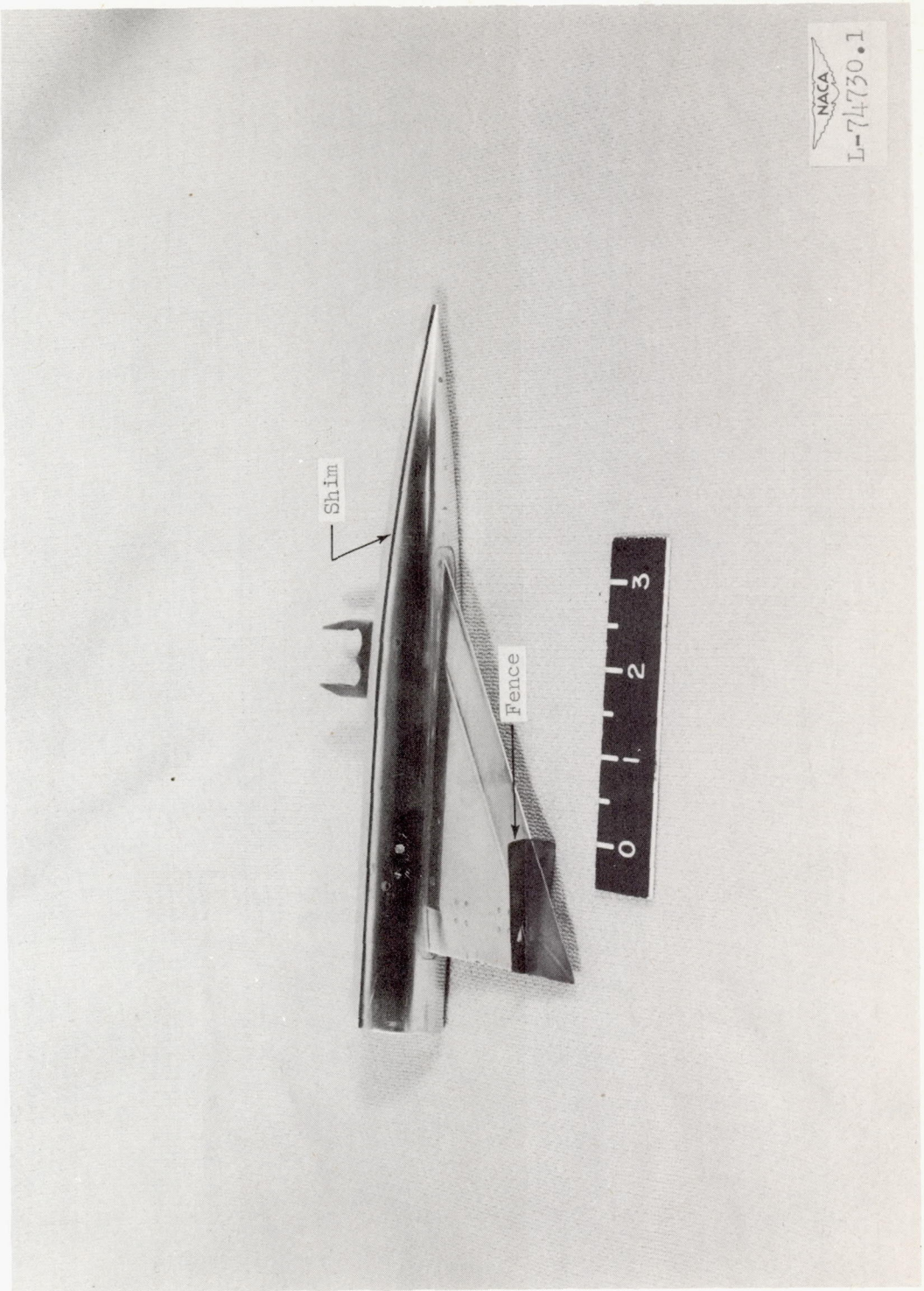

Figure 2.- Test model.

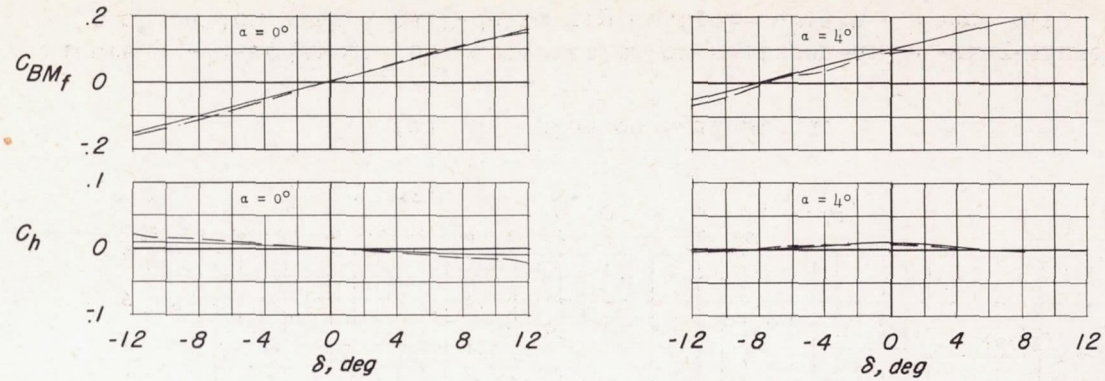

(a) Variation of C_{BM_f} and C_h with δ.

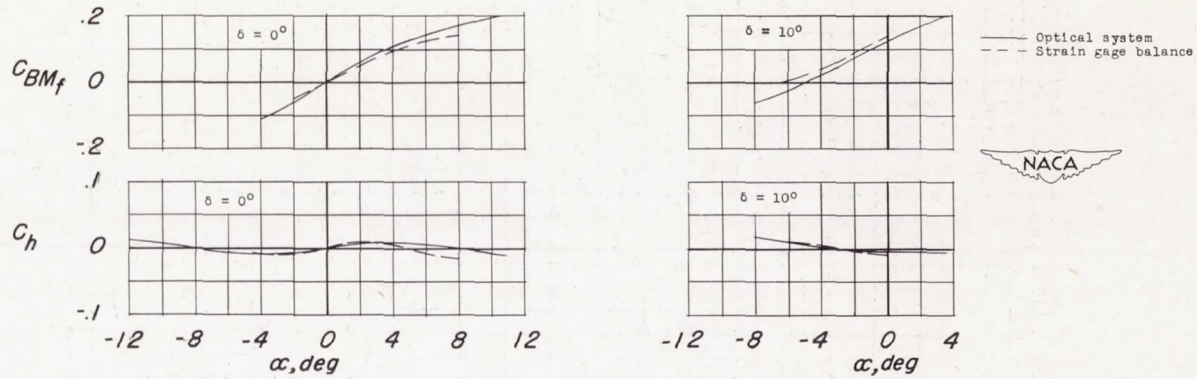

(b) Variation of C_{BM_f} and C_h with α.

Figure 3.- Comparison of hinge moment and bending moment of a tip control on a delta wing obtained by an optical system at M = 1.96 with results obtained by use of a strain-gage balance system at M = 1.90 (ref. 4).

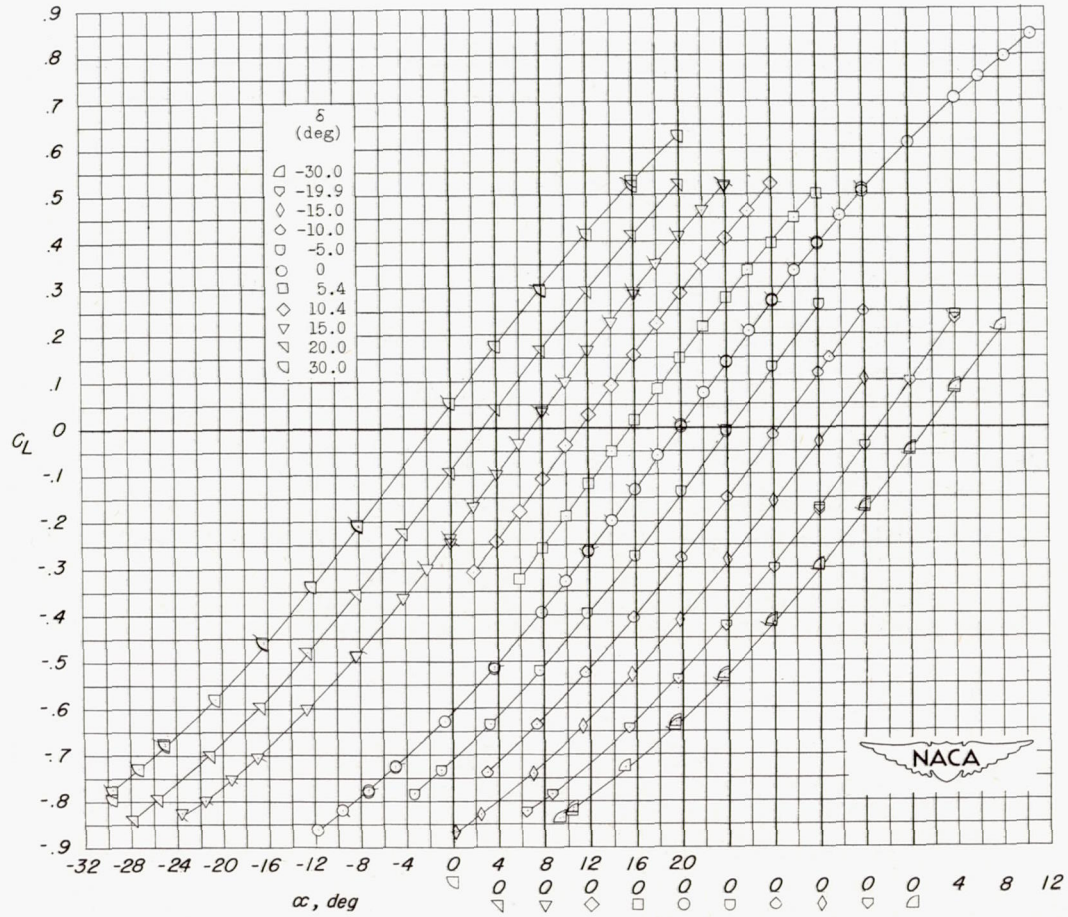

(a) C_L plotted against α.

Figure 4.- Aerodynamic characteristics of semispan-delta-wing—fuselage combination with a half-delta tip control surface. Fence off. $R = 2.0 \times 10^6$; $M = 1.96$. Flagged symbols denote repeat tests.

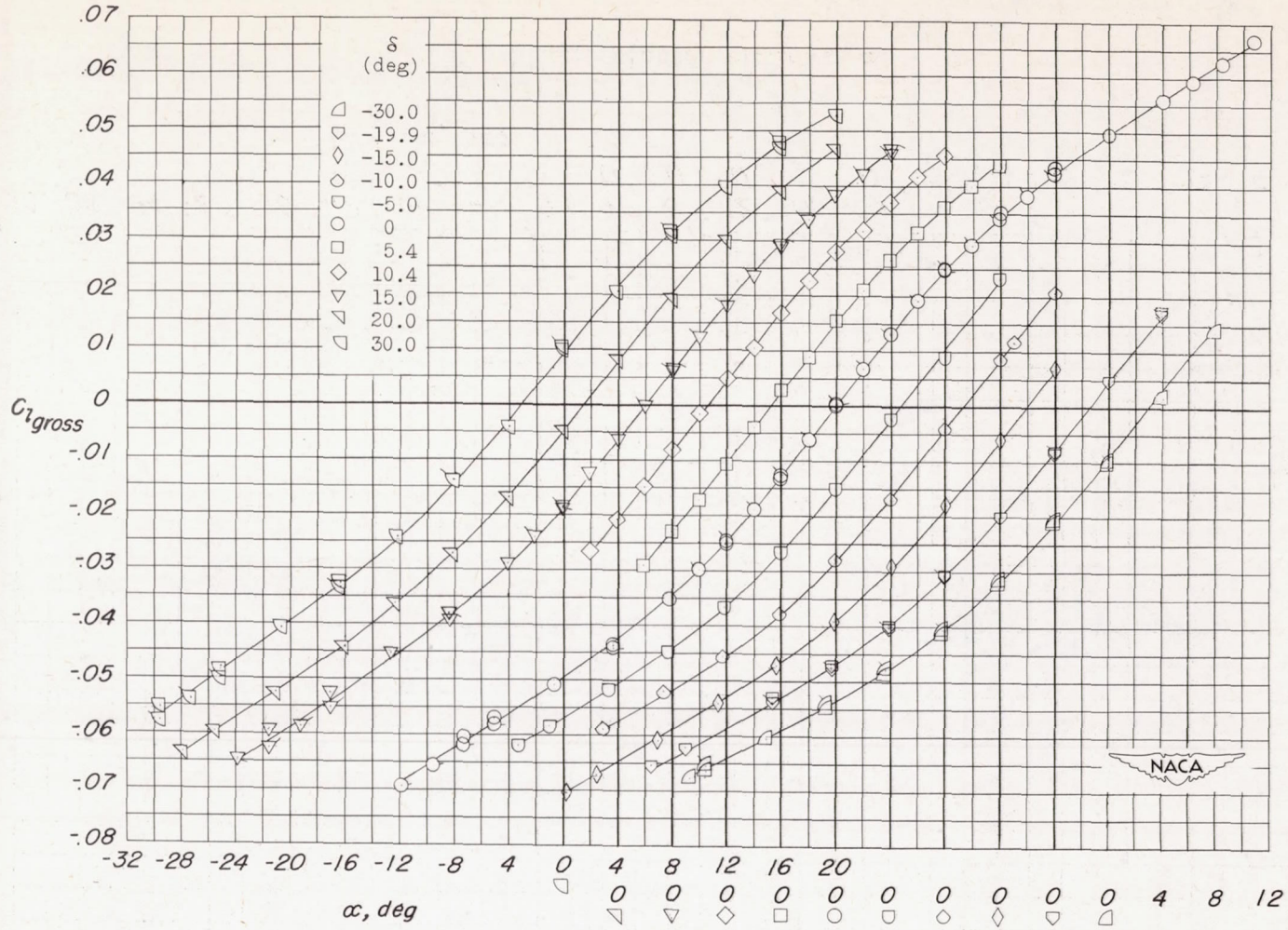

(b) $C_{l_{gross}}$ plotted against α.

Figure 4.- Continued.

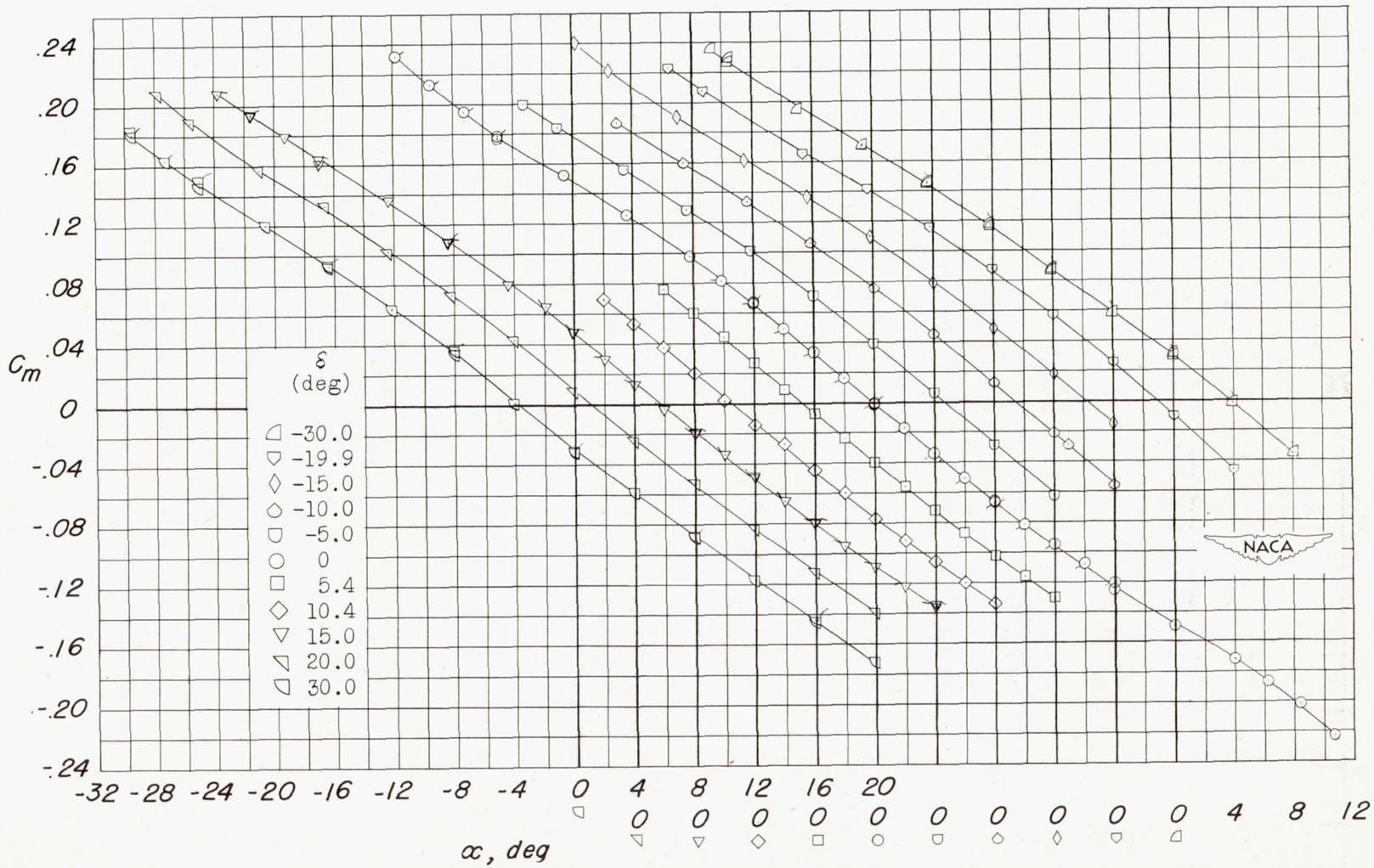

(c) C_m plotted against α.

Figure 4.- Continued.

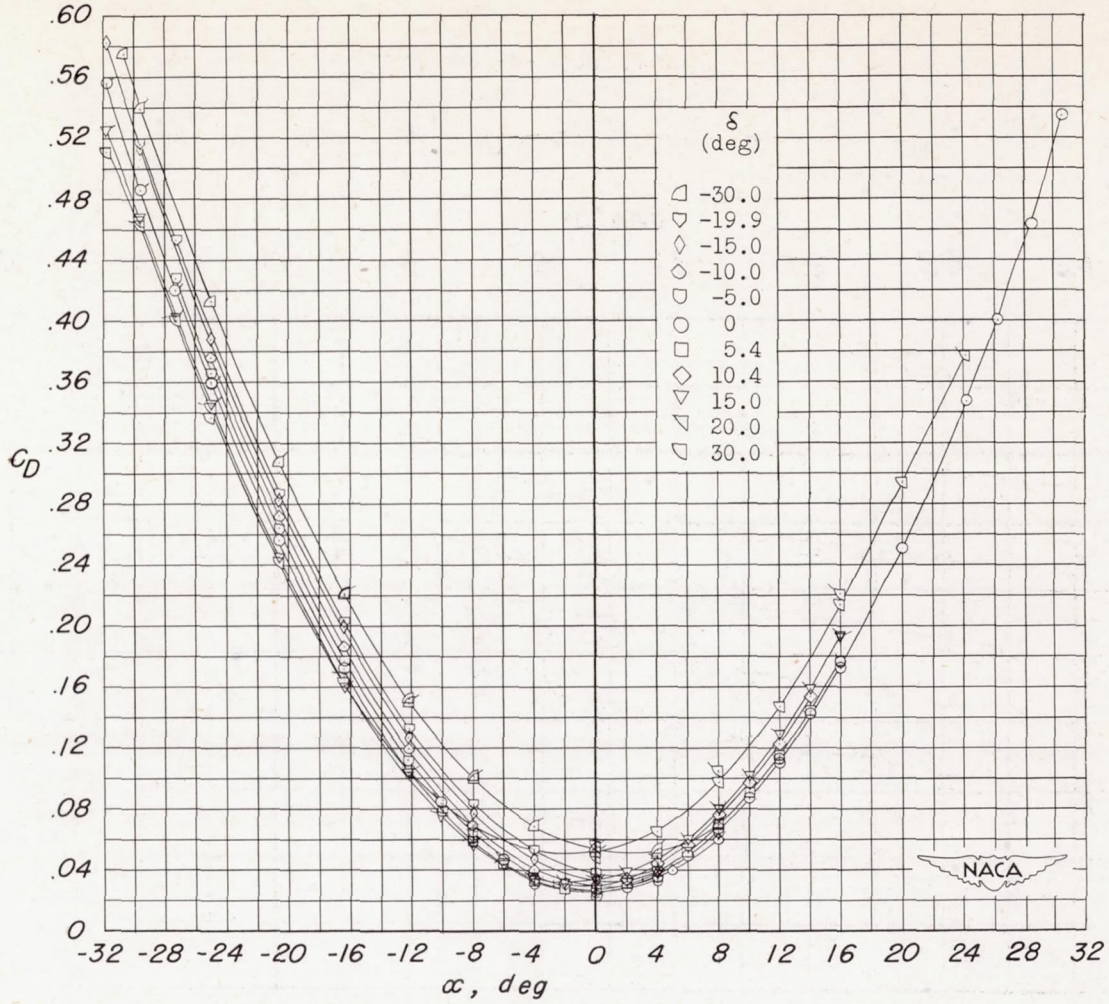

(d) C_D plotted against α.

Figure 4.- Continued.

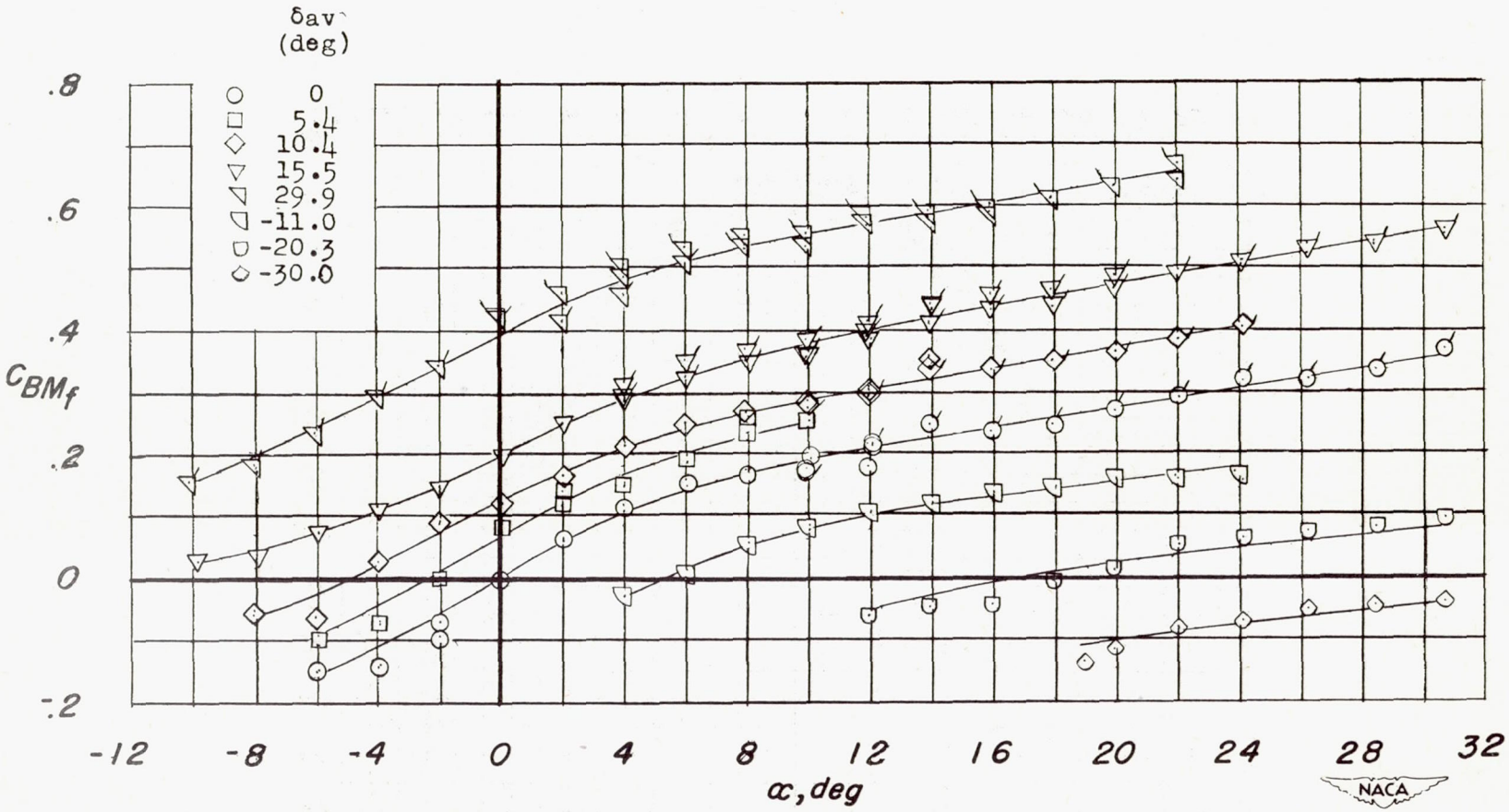

(e) C_{BM_f} plotted against α.

Figure 4.- Continued.

CONFIDENTIAL

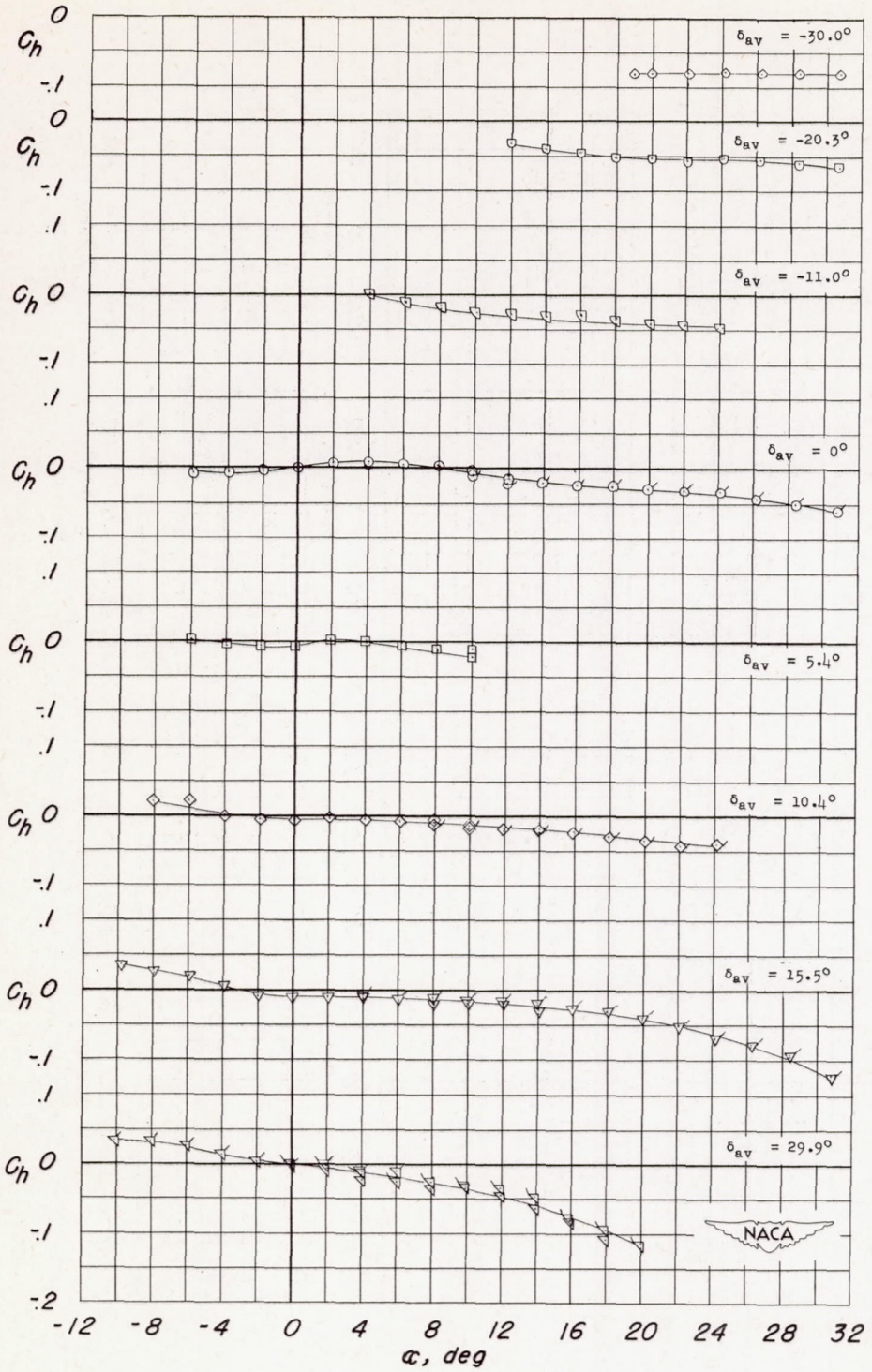

(f) C_h plotted against α.

Figure 4.- Concluded.

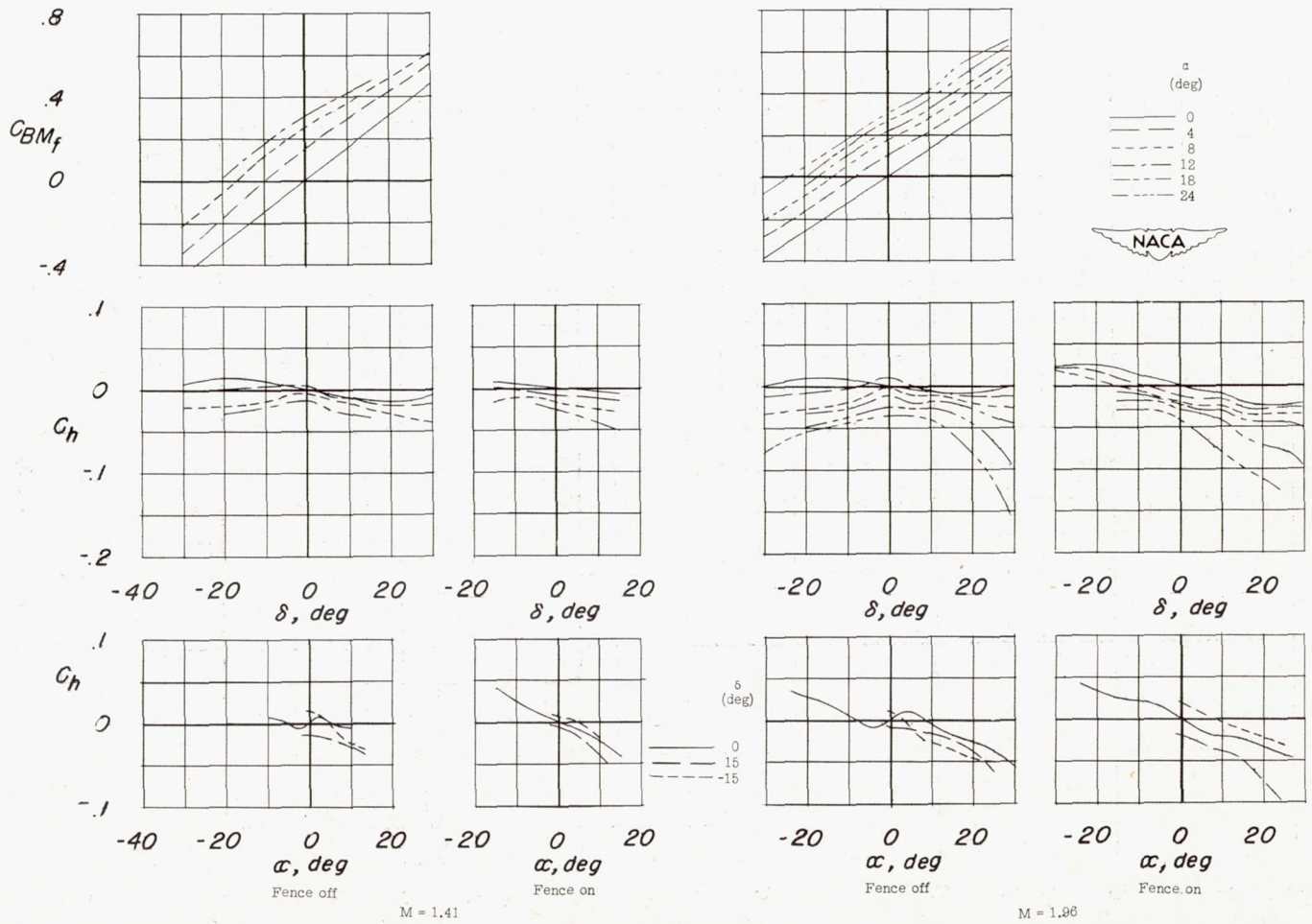

Figure 5.- Variation of control hinge moment and bending moment with control deflection and angle of attack. With and without fence. $R = 2.4 \times 10^6$ and $R = 2.0 \times 10^6$; M = 1.41 and M = 1.96, respectively.

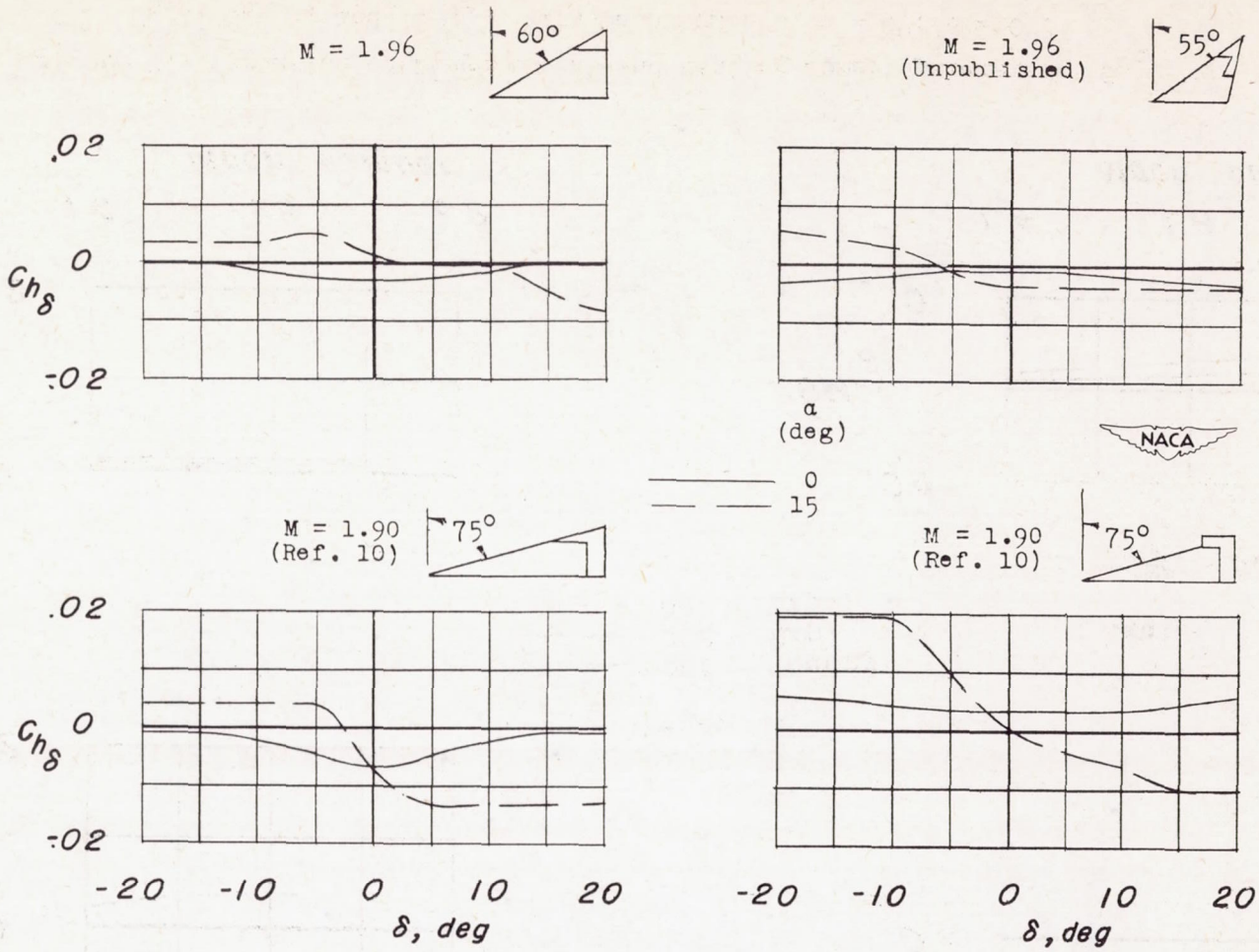

Figure 6.- Comparison of the variation with deflection of the parameter C_{h_δ} of the present investigation with that of three horn-balanced controls. Coefficients based on the control geometry behind the hinge line.

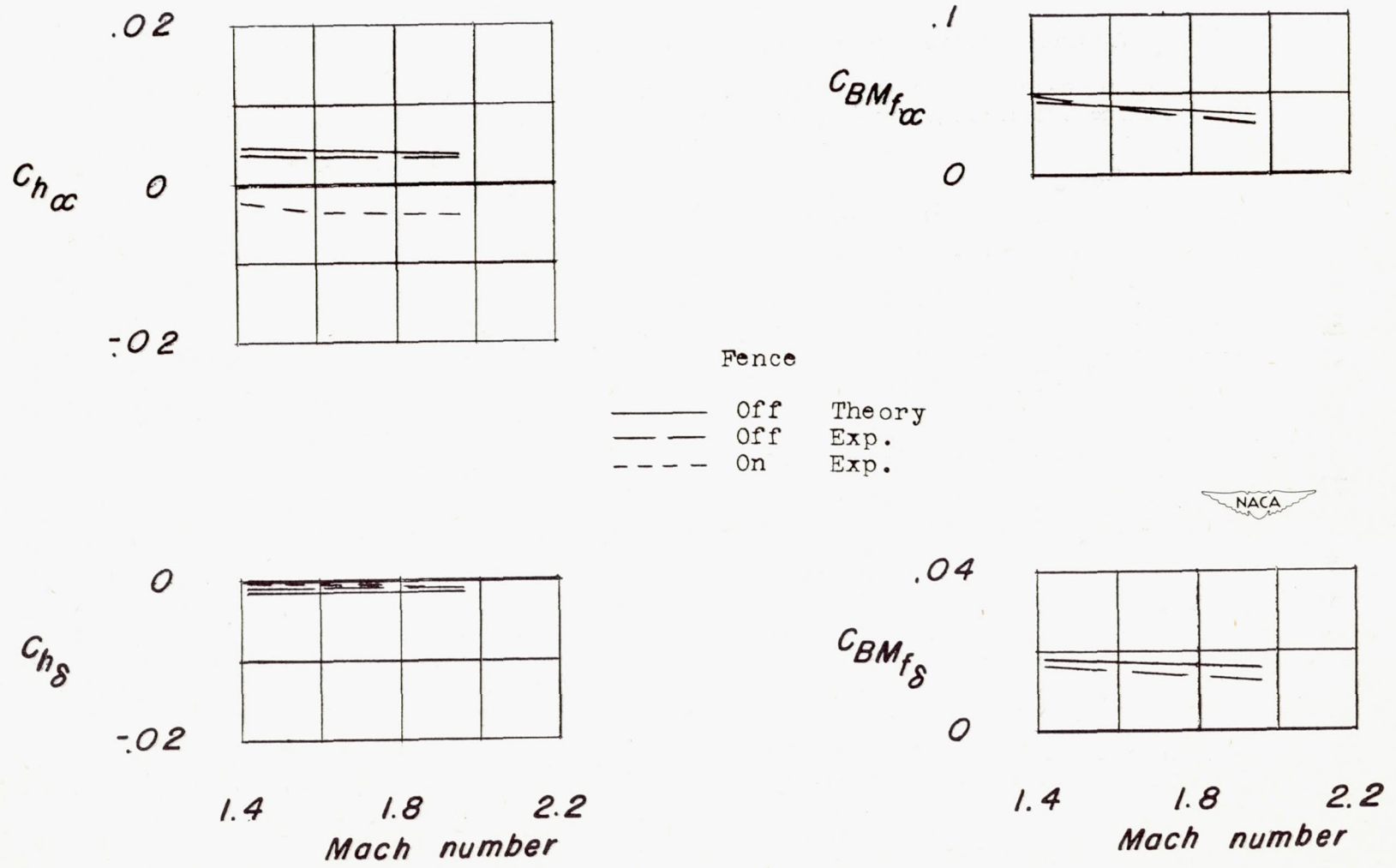

Figure 7.- Variation of hinge moment and bending-moment parameters C_{h_α}, C_{h_δ}, $C_{BM_{f_\alpha}}$, and $C_{BM_{f_\delta}}$ with Mach number. $\alpha = 0^\circ$; $\delta = 0^\circ$.

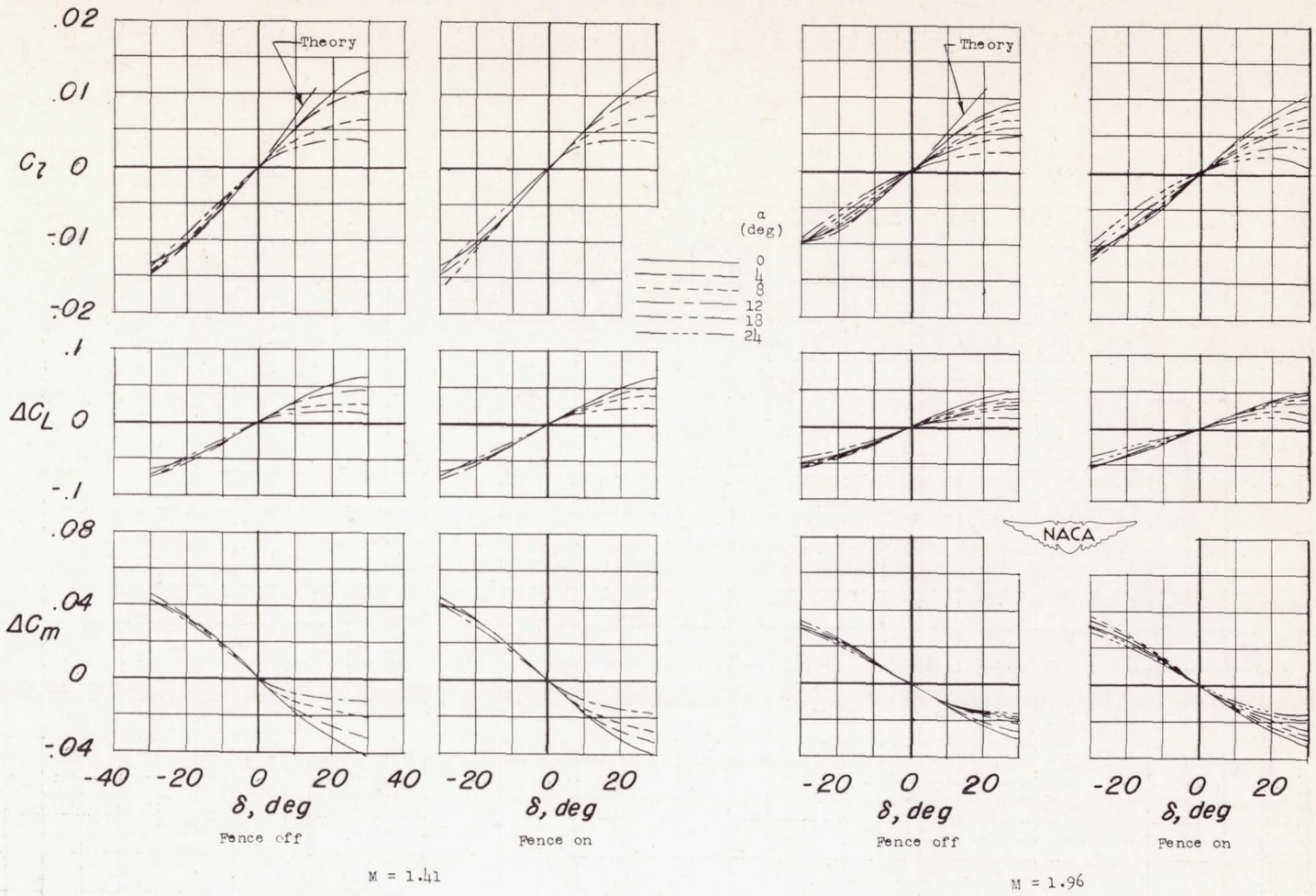

Figure 8.- Variation with deflection of rolling moment and the increments of lift and of pitching moment due to deflection. With and without fence. $R = 2.4 \times 10^6$ and $R = 2.0 \times 10^6$; M = 1.41 and M = 1.96, respectively.

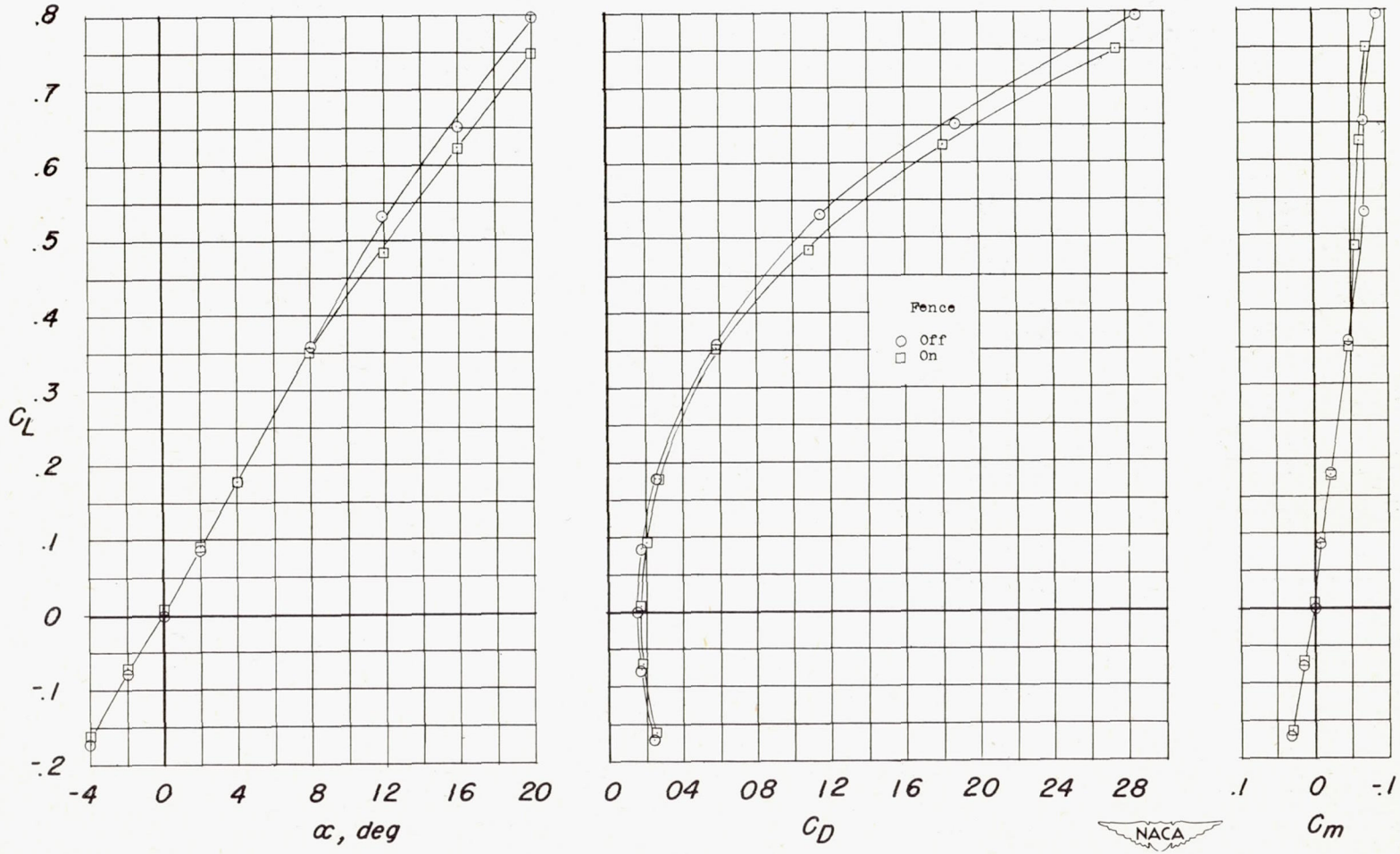

(a) M = 0.73; R = 2.3×10^6.

Figure 9.- Effects of a fence on the lift, drag, and pitching-moment characteristics of the wing-fuselage combination. $\delta = 0^\circ$.

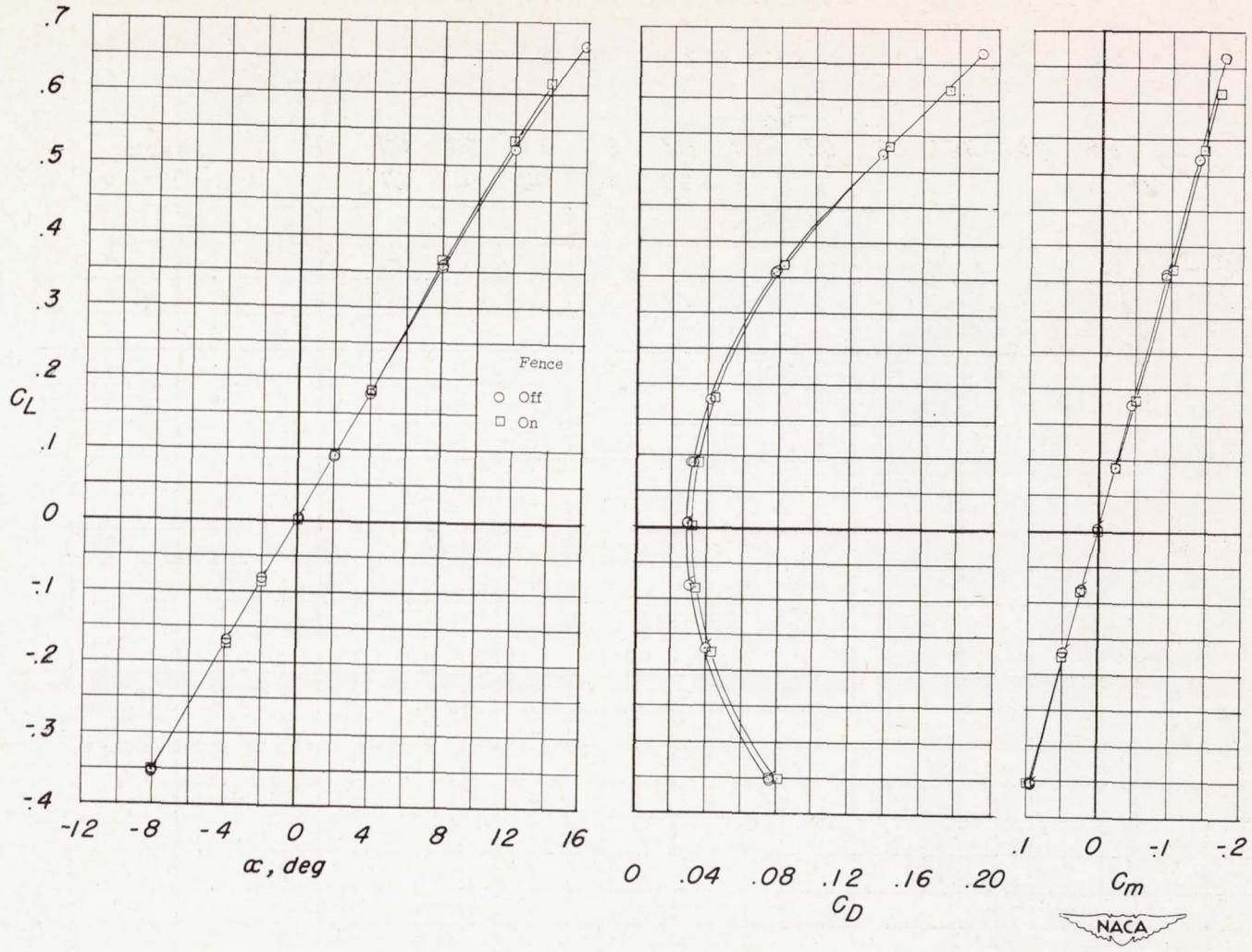

(b) M = 1.41; R = 2.4×10^6.

Figure 9.- Continued.

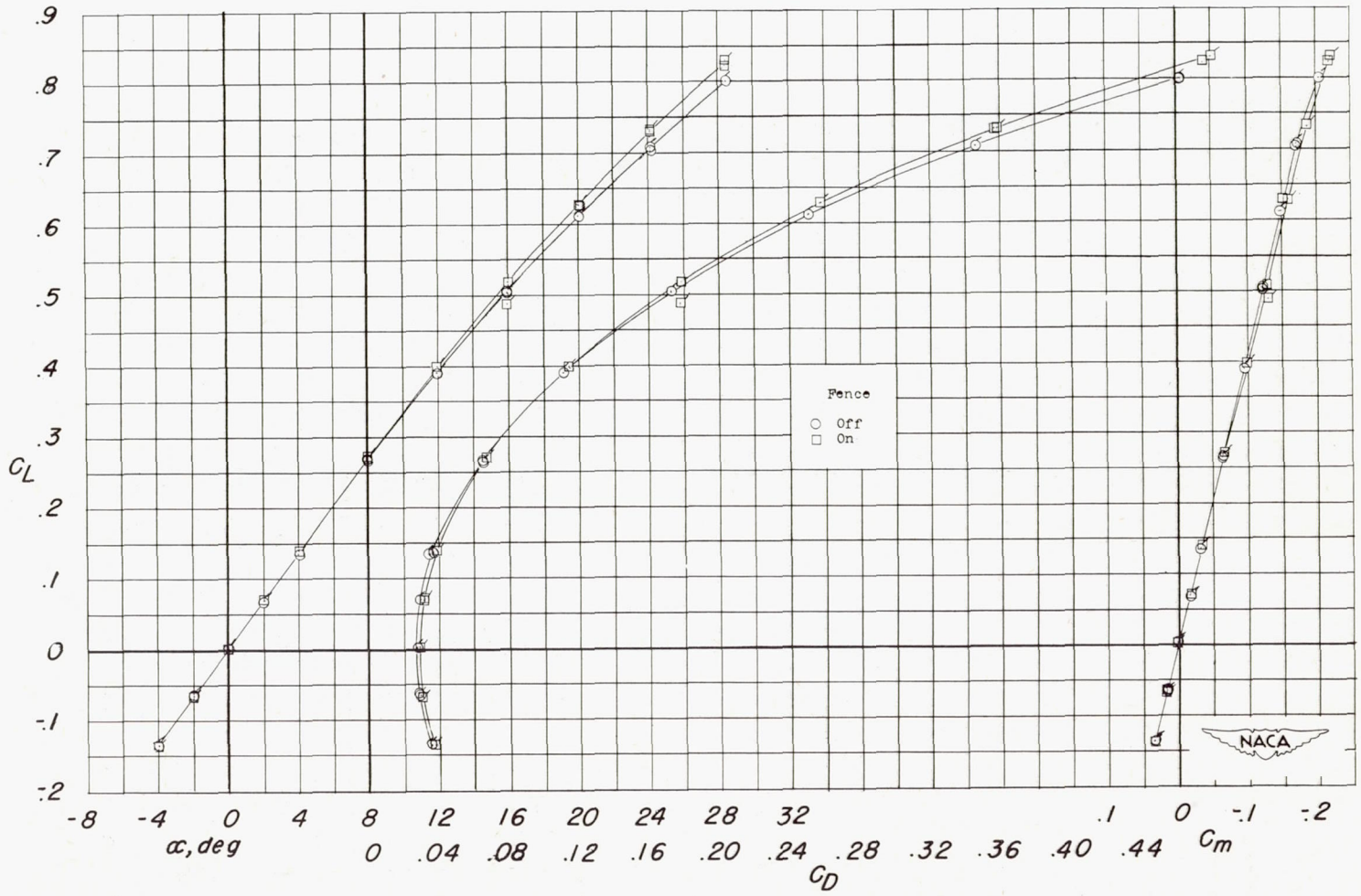

(c) M = 1.96; R = 2.0×10^6.

Figure 9.- Concluded.

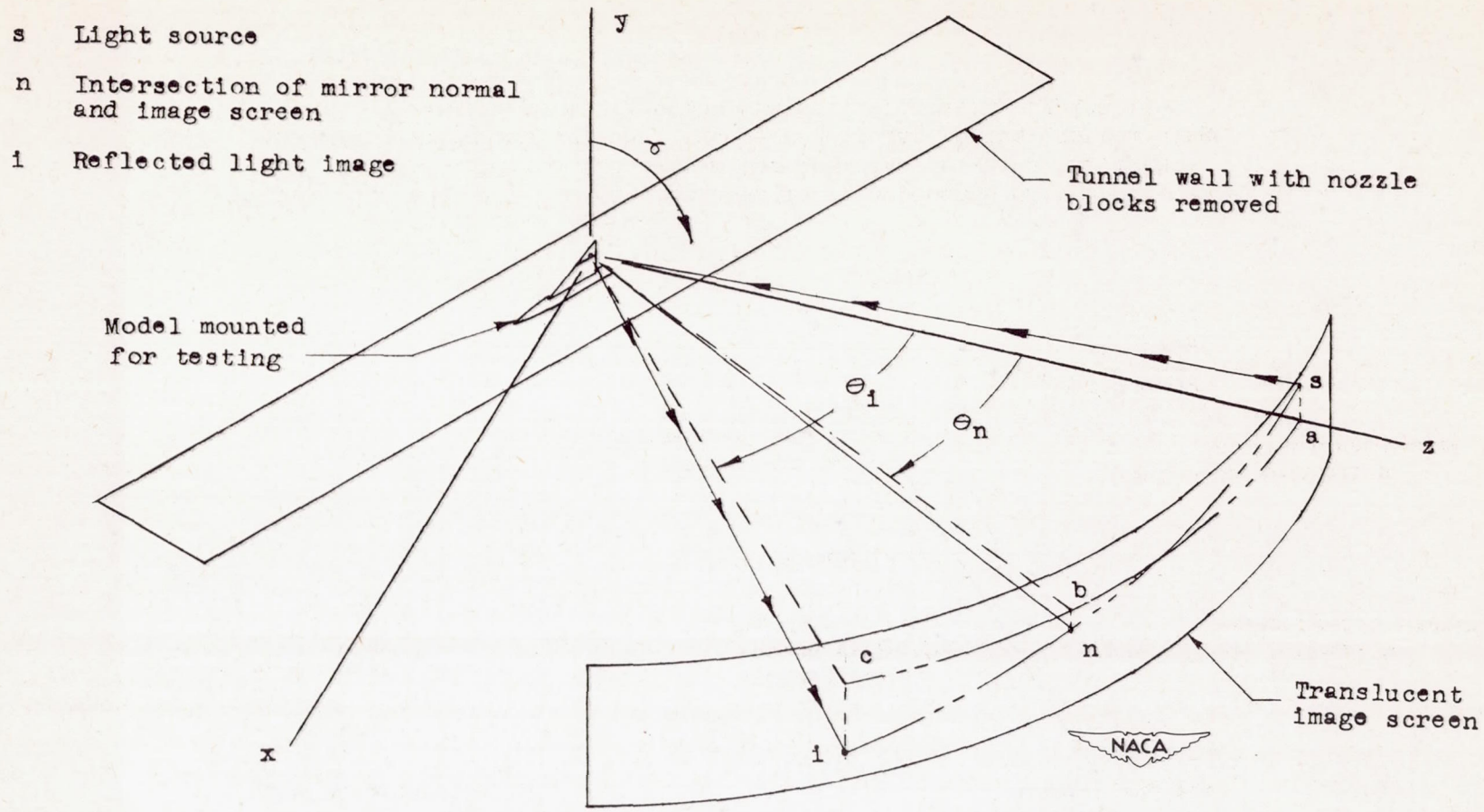

Figure 10.- General arrangement of optical system designed for use in the Langley 9- by 12-inch supersonic blowdown tunnel.

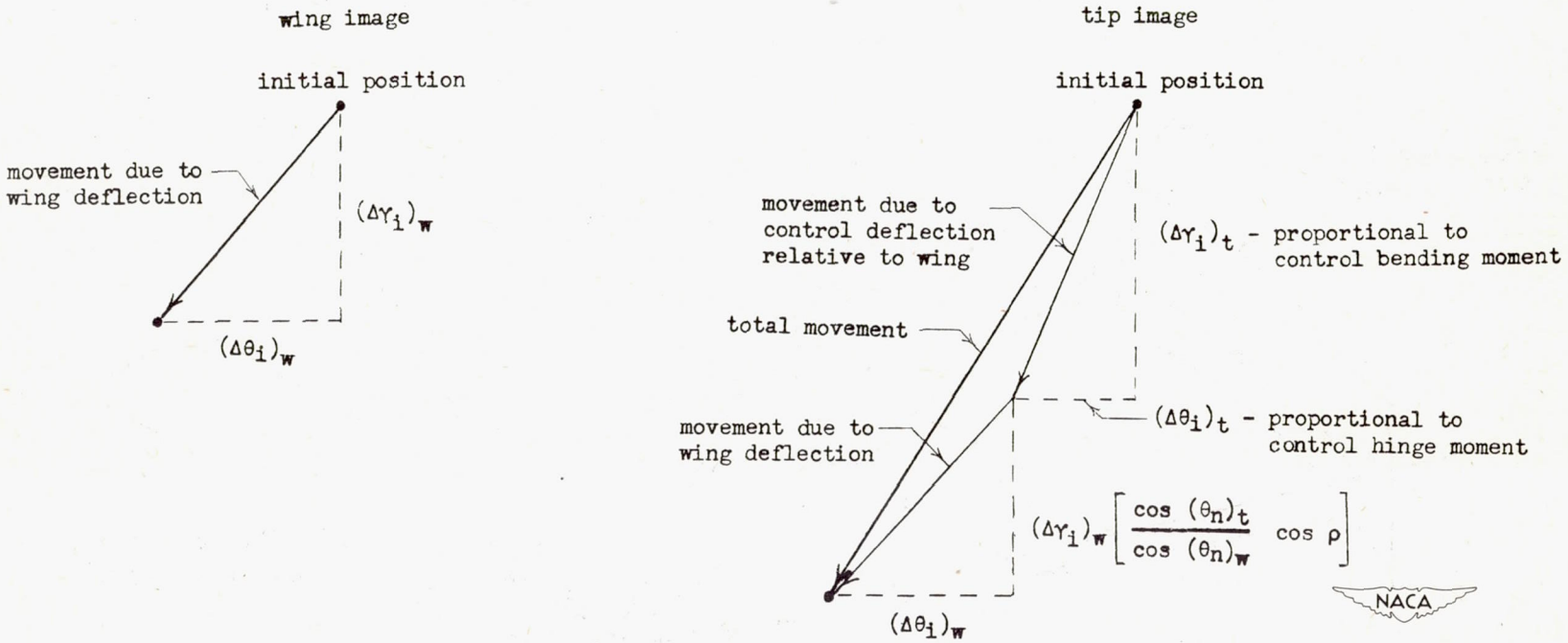

Figure 11.- Illustration of breakdown into components of the movements of images of the optical system for the case in which the light-mirror systems are coplanar and perpendicular to the control hinge axis. (Relative vector lengths are not necessarily typical.)

NACA-Langley - 10-14-52 - 350